POLITECNICO DI TORINO
Repository ISTITUZIONALE

Experimental investigation of the hydrodynamic performance of the ISWEC 1:20 scaled device

Original
Experimental investigation of the hydrodynamic performance of the ISWEC 1:20 scaled device / Sirigu, S.A., Bonfanti, M., Passione, B., Begovic, E., Bertorello, C., Dafnakis, P., Bracco, G., Giorcelli, E., Mattiazzo, G.. - ELETTRONICO. - (2018), pp. 551-560. (NAV 2018 Trieste 20 Giugno 2018) [10.3233/978-1-61499-870-9-551].

Availability:
This version is available at: 11583/2710055 since: 2018-06-25T14:45:52Z

Publisher:
IOS Press

Published
DOI:10.3233/978-1-61499-870-9-551

Terms of use:

This article is made available under terms and conditions as specified in the corresponding bibliographic description in the repository

Publisher copyright

(Article begins on next page)

06 November 2026

Technology and Science for the Ships of the Future
A. Marinò and V. Bucci (Eds.)
IOS Press, 2018

© 2018 The authors and IOS Press. All rights reserved.
doi:10.3233/978-1-61499-870-9-551

Experimental Investigation of the Hydrodynamic Performance of the ISWEC 1:20 Scaled Device

Sergej Antonello SIRIGU[a,1] Mauro BONFANTI [a] Biagio PASSIONE [a] Ermina BEGOVIC [b] Carlo BERTORELLO [b] Panagiotis DAFNAKIS [a] Giovanni BRACCO [a] Ermanno GIORCELLI [a] and Giuliana MATTIAZZO [a]
[a] *Politechnic of Turin*
[b] *University of Naples Federico II*

Abstract. An experimental campaign test has performed on the 1:20 scaled moored model of ISWEC (Inertial Sea Wave Energy Converter). The annual productivity of the device is strictly correlated to the hydrodynamic properties of the floater. Therefore, is fundamental to carry out an experimental investigation of the hydrodynamic performance of the floater and compare the results with the numerical codes. In this paper the experimental campaign is described. Two different mooring configurations were tested to understand the different influence of mooring forces on the floater dynamics. The non-dimensional Response Amplitude Operator (RAO) is representative of the hydrodynamic performances of the floater. Therefore, the device with both the mooring configurations has been tested in regular waves of constant wave steepness 1/50. Conclusions are commenting the differences a between numerical and experimental results and the impact of nonlinearities on hydrodynamic performances.

Keywords. Wave Energy Converter, ISWEC, hydrodynamics, Experimental, mooring system, RAO

1. Introduction

In floating wave energy converter field, the annual productivity of the devices is strictly correlated to the hydrodynamic properties of the floater. Numerical codes have been developed in these decades to simulate the floater dynamics under both regular and irregular waves [1], [2]. These software are based on 3-D boundary element method that solves the flow potential around the floater and are able to calculate the hydrodynamic characteristics of the body. Therefore, it is common to design and optimize the shape of the WEC through numerical simulation instead of carrying out experimental tests to reduce the conceptual phase costs [3]. The principal drawback of the numerical approach is the linear hypothesis of the potential flow theory. Therefore, the model is valid and reliable for low wave steepness and small oscillation of the floater. WECs are designed to work in resonance conditions and to extract as much energy as possible from the incoming waves and then the linear hypothesis is no longer satisfied. When the floater

[1] Sergej Antonello Sirigu, Department of Mechanical and Aerospace Engineering, Politechnic of Turin, Corso Duca degli Abruzzi 24, Turin , Italy; E-mail: sergej.sirigu@polito.it.

motion or oscillation becomes important, viscous and non-linear effects start to play a fundamental role in the WEC dynamics [4]. Moreover, the WEC is supposed to be moored on the seabed [5], and this condition lead to another source of non-linearity.

After the preliminary designing process of the WEC is necessary to carry out experimental tests on the scaled device in order to describe and understand the real behaviour of the floater in real waves. During an experimental campaign important information can be analysed to improve the design of the device: the real performances of the floater, the dynamic behaviour of the mooring system, the analysis of mooring loads in extreme conditions etc. [6].

In this paper the experimental test campaign of the ISWEC device for regular waves is presented. ISWEC is a pitching floating device that exploit the energy of the incoming wave through a gyroscopic system installed inside a sealed hull [7]. The device is slack moored on the sea bed with a mooring system designed to weathervane and thus work in head seas. The numerical model of the device and its numerical optimization algorithm is discussed in [8]. A full-scale prototype has been tested in Pantelleria Island in 2015 [9]. Focus of this work is the description of the 1:20 scaling down of the device, the description of the experimental tests and the determination of the Response Amplitude Operator for two versions of a new mooring system configuration.

2. Model preparation

2.1. Model

To validate the performances of the ISWEC fullscale device designed for the Pantelleria Island site an experimental campaign on a 1:20 model was performed in the wave tank

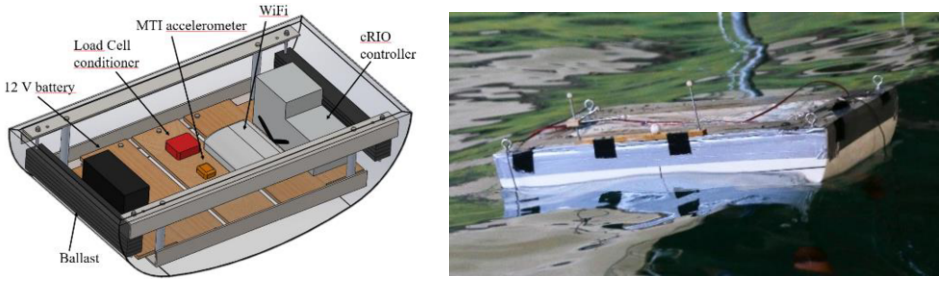


Figure 1. From left: a) CAD of the device with functional components b) picture of the device during tests.

of University of Naples Federico II. The geometrical and inertial properties of the device have been scaled according to the Froude law. Full scale properties with its corresponding scaled values are shown in Table 1in comparison to the measured values. The experimental values of inertias and COG were obtained using an inertial balance present in the wave tank facility.

Table 1. Full scale and 1:20 model geometrical and inertial properties.

Data	Full scale model	1:20 scaled model	1:20 scaled experimental model
Length (m)	15.3	0.767	0.767
Width (m)	8.0	0.4	0.4
Height (m)	4.5	0.225	0.225
Mass (kg)	288090	36	36
COG from waterlevel (m)	-0.53	-0.027	-0.028
COG from deck (m)	2.03	0.102	0.104
I_{xx} (kg*m^2)	1923000	0.6	0.56
I_{yy} (kg*m^2)	8486000	2.65	2.41
I_{zz} (kg*m^2)	7150000	2.23	-
Draft (m)	3.0	0.15	0.15

2.2. Mooring configurations

In this experimental campaign two different mooring system configurations were tested. The mooring configurations consists essentially in 3 chain lines anchored to the artificial seabed and connected to a central joint. Two chain bridles connect the device to a mechanical swivel and there are three jumpers connected to each main mooring line to assure the desired mooring stiffness. The mooring system is designed to allow the weathervaning of the device, to influence as little as possible the pitch motion and to present a satisfying behavior in extreme weather conditions.

The dynamic behavior of this system is principally governed by the gravity and inertia forces Therefore, the mooring system was scaled also with Froude scaling law with the scaling factor $\lambda = 1/20$.

Figure 2 shows the two mooring configurations C1 and C2a tested in the experimental campaign. The difference between the configuration C1 and C2a is the presence of the clump weight in the configuration C2a to increase the mooring stiffness. The jumpers net buoyancies and volumes are designed to lift the weight of 1.1 m of chain in water in both configurations.

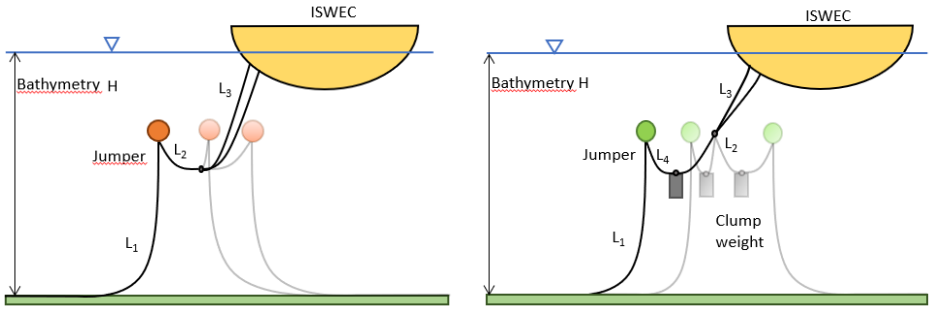


Figure 2. From left: a) Mooring C1 configuration. b) Mooring C2a configuration.

A Genovese type chain was used to make the mooring lines, and the properties are shown in Table 2. The properties of the mooring configurations for both 1:20 model and full-scale device are resumed in Table 3 and Table 4.

Table 2. Mooring chains properties – Genovese type.

Variable	Bridle - Full scale model	Bridle - Scaled model	Bottom mooring - Full scale model	Bottom mooring - Scaled model
Diameter wire (mm)	44.0	2.2	60	3.0
Weight per meter (kg/m)	36	0.09	74.4	0.186
Weight per meter in water (kg/m)	32	0.08	68.8	0.172

Table 3. C1 Mooring configuration characteristics.

Mooring property	Full scale model	1:20 scaled model
Bathymetry, H (m)	25	1.25
Anchor – Jumper length, L1 (m)	65	3.25
Jumper – Bridle length, L2 (m)	10	0.5
Bridle – Model length, L3 (m)	10	0.5
Jumper net buoyancy, B (kg)	1512	0.189

Table 4. C2a Mooring configuration characteristics.

Mooring property	Full scale model	1:20 scaled model
Bathymetry, H (m)	25	1.25
Anchor – Jumper length, L1 (m)	65	3.25
Clump weight – Bridle length, L2 (m)	10	0.5
Bridle – Model length, L3 (m)	10	0.5
Jumper – Clump weight length, L4 (m)	5.0	0.25
Jumper net buoyancy, B (kg)	3615	0.452
Clump weight, G (kg)	2000	0.250

3. Facility and experimental setup

This chapter concerns on a brief description of the experimental setup performed for all experimental tests in the towing tank of the University Federico II. A summary of the main characteristics of the test tank will be followed by an accurate description of the sensor and its acquisition systems.

3.1. Federico II wave tank

The towing tank of the Department of Industrial Engineering of the University Federico II is 136.74 m long, 9 m wide and 4.25 m deep. The wave maker is multi flap type, by Edinburgh Design. Each of the eight pads, 2x1.125 m is electro-hydraulically powered, with maximum excursion amplitude of about ±20 deg.

The wave-maker is able to generate regular waves in frequency range 0.2 – 1.25 Hz, with the maximum wave height up to 0.48m, standard theoretic and spectra and user defined time series. Moreover, the towing tank is equipped with a movable carriage carrying the data acquisition system.

3.2. Wave probes

Encounter waves were measured by two ultrasonic gauges WP1 and WP2, and one Capacitive gauge WP3, one located on the tank side at 3.9 m laterally from the device, the other two at centreline, 3.2 m ahead from CG. With reference to Figure 3, the three probes are positioned in such a way as to acquire the wave field at different points of the tank in order to better describe the evolution of the wave height over time. The gauges transmit the collected data to the data acquisition and processing system.

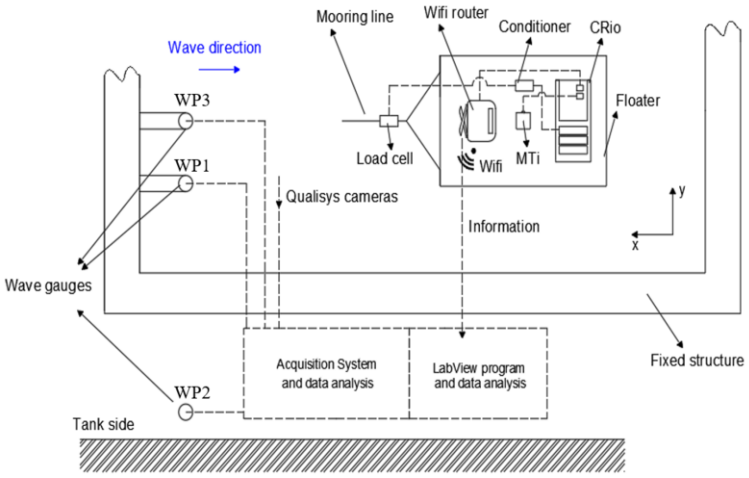


Figure 3. Experimental setup, sensors and acquisition system.

3.3. Qualisys motion tracking

Two different motion acquisition systems were used during the tests: a motion tracking system (QualiSys) and an inertial unit of measurement (IMU). The QualiSys system tracks the motion of a rigid body through a system of cameras that identify the motion of 4 reflecting markers positioned on the device deck that identify the global position of the body (shown in Figure 3). The markers positions are recorded by the cameras and elaborated by a dedicated software that gives in output the six DoF motions of the body.

3.4. Artificial sea bed

To ensure a correspondence between the configuration of the moored scale prototype and therefore the scalability of the results, artificial sea-beds have been used to recreate the depth of the site where the full-scale prototype will be deployed. The artificial sea-beds were made using steel bars and PVC pipes connected by orthogonal joints in order to create the structure shown in Figure 4. The seabed was built using a plastic grid stretched to ensure as much as possible its flatness.

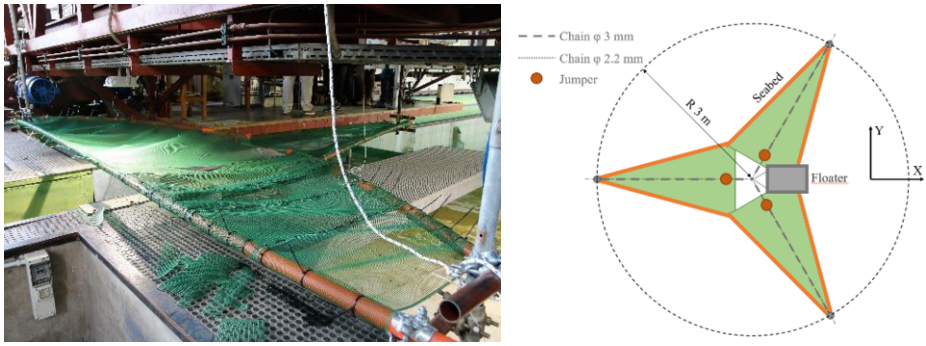


Figure 4. From left: a) picture of the artificial sea bed mounted on the movable carriage b) top view sketch of the artificial sea bed and mooring lines.

3.5. On-Board instrumentation

On-board instrumentation was implemented for the measurements of the angular motions of the floater via an MTI system and for the mooring load cell. The purpose of having an MTI system on-board is to compare the MTI measurements with the QualiSys system and to provide a redundancy in the motion acquisition.

The MTI is fixed inside the hull, appropriately mounted to have the internal reference system oriented like the hull reference system. As shown in Figure 3, the inertial sensor transmits data via RS232 serial connection to the CompactRio system (cRIO). The latter, connected to a Wifi router, was in charge of data acquisition and transmission to a laptop PC where the data was saved using a LabView program in txt format.

The load cell is connected on one side to the two bridles of the mooring and on the other to the chain connecting the two branches to the jumper. The load cell is connected to a conditioner which amplifies the signal and transmits it to the cRIO via analog output connection.

3.6. Data processing

Standard data processing, cleaning and filtering were used on the experimental data. The first operation is the elimination of any eventual spike and missing data through and adequate median filter. The data is subsequently filtered with a Butterworth low-pass filter with a frequency cut-off of 10 Hz, ten times the characteristic frequency of the physical phenomenon in order to eliminate the measurement chain noise.

The choice of which time interval to analyse is fundamental for a consistent data analysis. In Figure 5 an example of processed data for the 6 DoF of the floater and chosen time interval for the analysis is shown. For every test the time interval is chosen where the motion is more stationary. An FFT analysis is then carried out to obtain the signal frequency and amplitude of each floater DoF measured by QualiSys system and wave probe measurement.

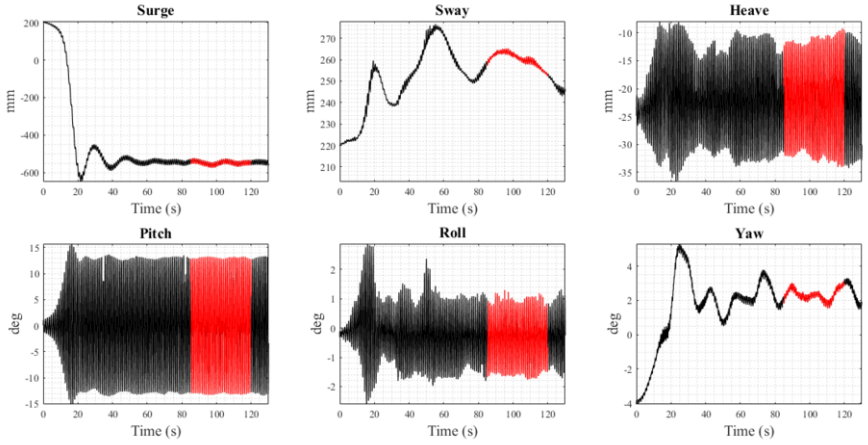


Figure 5. time series of the DoFs motion of the floater during a regular wave test with T = 0.952 s, a = 17,2 mm. In red the chosen interval for the FFT elaboration.

4. Results

In this experimental campaign different test typologies were carried out to investigate the hydrodynamic behaviour of the moored floater. In this paper the results concerning the static and in regular waves conditions of the two mooring system will be presented and discussed.

4.1. Mooring static characteristics

The mooring static characteristics for both mooring configurations C1 and C2a were calculated from the experimental data: the load cell measured the static force and the QualiSys system measured the distance of the floater from the anchor. A pull-out test was performed in absence of incoming waves. starting from the equilibrium condition at the centre of the mooring system, the device was pulled away along the direction of one of the three mooring lines and the restoring force was measured every step of 2 cm. This procedure was repeated until the mooring line became fully stretched along the x direction as shown in Figure 4b.

The numerical static characteristics was obtained with Ansys Aqwa software. In Figure 6 the experimental and numerical static characteristics for both mooring configurations are shown.

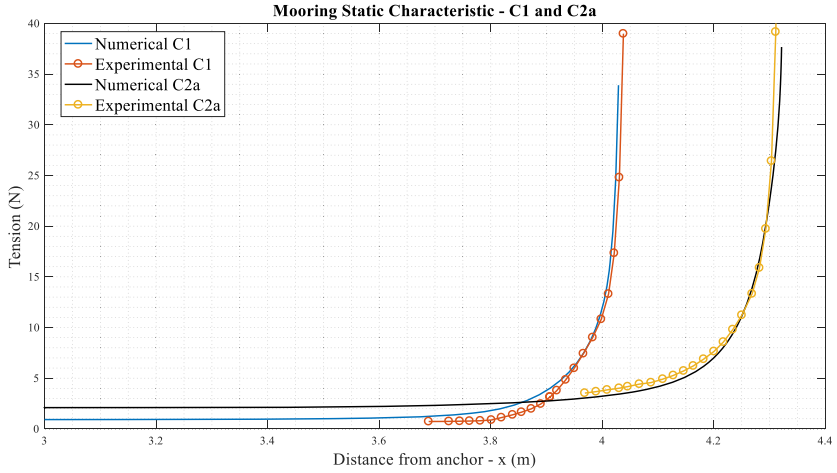


Figure 6. Experimental and numerical static characteristics of mooring system configation C1 and C2a.

There is a good agreement between numerical and experimental results. Mooring C2a present a higher stiffness and maximum elongation due to the presence of the clump weight and the additional chain length L_4 as shown in Table 4. Therefore, mooring configuration C2a has a higher capacity of absorbing the wave loads due to the larger area under the curve.

4.2. Regular Waves Test

In this section the results regarding the moored device in regular waves are presented. The device is tested in regular waves with a wave steepness of 1/50 for both mooring configurations. The complete list of tests is listed in Table 5.

For the experimental tests three wave probes were positioned as shown in Figure 3: WP1 and WP3 are positioned upstream of the device at the same coordinate y, the WP2 is mounted between the device and the tank wall.

Table 5. Regular wave list – wave steepness 1/50.

Freq (Hz)	a (mm)	Mooring C1	Mooring C2a
1.25	10.0	✓	✓
1.2	10.8	✓	✓
1.118	12.5	✓	✓
1.052	14.1	✓	✓
0.994	15.8	✓	✓
0.952	17.2	✓	✓
0.894	19.5	✓	✓
0.745	28.1	✓	✓
0.639	38.2	✓	✓
0.559	50.0	✓	✓
0.497	63.2	✓	X
0.447	78.1	✓	X

The RAOs evaluation was performed considering the mean value of the three wave probes amplitudes and it is defined as:

$$RAO_5 = \frac{\zeta_5}{ka} \tag{1}$$

Where ζ_5 is the pitch amplitude a, k is the wave number and a is the mean wave probe amplitude.

The non-dimensional pitch RAOs for both mooring configurations C1 and C2a are shown in Figure 7. The numerical RAO is calculated in zero-forward speed and no-mooring condition.

The RAO of the configuration C2a shows lower values in comparison to the configuration C1: configuration C2a is stiffer than C1 due to the presence of the clump weight as explained in section 4.1. The difference is bigger for the wave periods close to the natural period of the floater where the drift forces are higher and therefore the mooring forces increase.

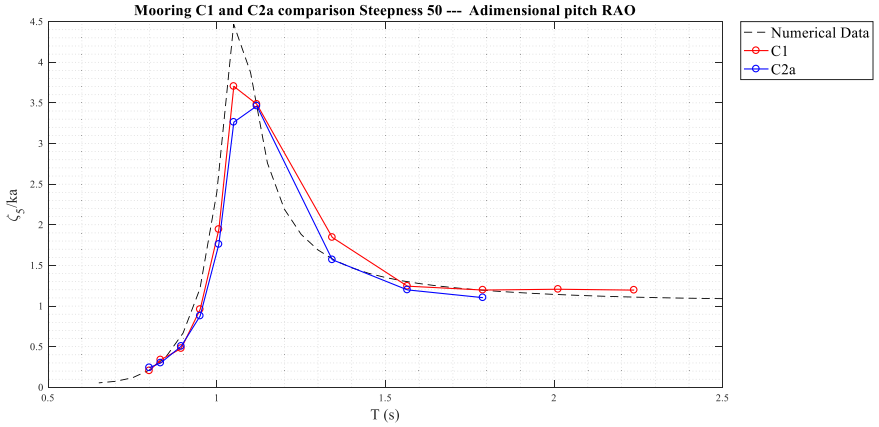


Figure 7. Non-dimensional pitch RAO for the two different mooring configurations C1 and C2a – Wave steepness 1/50.

Moreover, the experimental RAO is compared with the numerical RAO calculated with Ansys Aqwa. The numerical RAO is representative of the real dynamic behaviour of the device. The difference between the numerical and experimental is more relevant close to the pitch natural period where the oscillation is high and the linear theory is not enough to describe the floater dynamics: the viscous damping and drift forces become important, and therefore also the mooring forces.

5. Conclusions

The first results of the experimental campaign on the 1:20 ISWEC scaled model carried out in the towing tank of University of Naples Federico II have been presented and discussed. Two variations of a mooring configuration were studied and compared. The experimental static characteristics of the two mooring systems are in agreement with the

numerical simulations results and mooring C2a shows a higher capacity of energy absorption but with the drawback of increasing the mooring loads on the hull.

This drawback can be notice studying the behaviour of the floater in regular waves. The Response Amplitude Operator was calculated for both mooring configurations for the same wave steepness. Mooring configuration C2a shows lower performances close to the pitch natural period of the floater, where the drift forces are higher. Therefore, the annual productivity of configuration C2a will be lower than C1. The choose of the mooring system is a compromise between energy extraction performances and survivability capabilities. The numerical RAO shows a good agreement with the experimental values. Close to the natural period the experimental curve has lower values than the numerical one, due to the increase in importance of the non-linear contributions of viscous and mooring loads.

Further work on the experimental data will be carried out. Viscous and linear damping will be identify analysing the free decay data for both pitch and roll DoF. The dynamics of the two mooring systems under extreme condition will be studied.

Moreover, the numerical RAO considering also the mooring dynamics will be simulated in Ansys Aqwa environment and compared with the experimental results in order to validate the numerical design tool.

References

[1] M. Penalba, Using NEMOH for Modelling Wave Energy Converters: A Comparative Study with WAMIT, *12th European Wave and Tidal Energy Conference*, Cork, (2017).

[2] J. Pastor, Frequency and time domain modeling and power output for a heaving point absorber wave energy converter, *International Journal of Energy and Environmental Engineering*, (2014), 5:101.

[3] J. Goggins, Shape optimisation of floating wave energy converters for a specified wave energy spectrum, *Renewable Energy*, **71**, (2014), 208-220.

[4] M. Penalba, A Review of Non-Linear Approaches for Wave Energy Converter Modelling, *Proceedings of the 11th European Wave and Tidal Energy Conference 6-11th*, (2015), Nantes, France.

[5] R.E. Harris, Mooring systems for wave energy converters: A review of design issues and choices, *Proceedings of the Institution of Mechanical Engineers Part B Journal of Engineering Manufacture*, **220(4)**, (2006), 159-168.

[6] W.Sheng, Experimental Investigation of Hydrodynamic Characteristics of a Moored Floating WEC, *3rd International Conference on Ocean Energy*, (2010), Bilbao

[7] G. Bracco, Performance assessment of the full scale ISWEC system, *Proceedings of the IEEE International Conference on Industrial Technology*, art no. 7125466, (2015), 2499-2505.

[8] S.A. Sirigu, ISWEC design tool, *International Journal of Marine Energy*, **15**, (2016), 201-213.

[9] A. Cagninei, Productivity analysis of the full scale inertial sea wave energy converter prototype: A test case in Pantelleria Island, *Journal of Renewable and Sustainable Energy*, **7 (6)**, (2015).